NAVAL POSTGRADUATE SCHOOL
Monterey, California

THESIS

OPTIMIZATION OF A HOLOGRAPHIC RECONSTRUCTION PROCESS FOR COMBUSTION PHENOMENA

by

Marcus A. McInnis

December 1982

Thesis Advisor: D. W. Netzer

Approved for public release; distribution unlimited

REPORT DOCUMENTATION PAGE

READ INSTRUCTIONS BEFORE COMPLETING FORM

1. REPORT NUMBER	2. GOVT ACCESSION NO. / 3. RECIPIENT'S CATALOG NUMBER
4. TITLE (and Subtitle): Optimization of a Holographic Reconstruction Process for Combustion Phenomena	5. TYPE OF REPORT & PERIOD COVERED: Master's Thesis, December 1982
	6. PERFORMING ORG. REPORT NUMBER
7. AUTHOR(s): Marcus A. McInnis	8. CONTRACT OR GRANT NUMBER(s)
9. PERFORMING ORGANIZATION NAME AND ADDRESS: Naval Postgraduate School, Monterey, California 93940	10. PROGRAM ELEMENT, PROJECT, TASK AREA & WORK UNIT NUMBERS
11. CONTROLLING OFFICE NAME AND ADDRESS: Naval Postgraduate School, Monterey, California 93940	12. REPORT DATE: December 1982
	13. NUMBER OF PAGES: 53
14. MONITORING AGENCY NAME & ADDRESS (if different from Controlling Office)	15. SECURITY CLASS. (of this report): Unclassified
	15a. DECLASSIFICATION/DOWNGRADING SCHEDULE

16. DISTRIBUTION STATEMENT (of this Report)

Approved for public release; distribution unlimited

17. DISTRIBUTION STATEMENT (of the abstract entered in Block 20, if different from Report)

18. SUPPLEMENTARY NOTES

19. KEY WORDS (Continue on reverse side if necessary and identify by block number)

pulsed ruby (.6943) laser illumination
Krypton (.6471) laser reconstruction
diffuse hologram
speckle suppression

20. ABSTRACT (Continue on reverse side if necessary and identify by block number)

This investigation addressed the resolution limiting speckle created in diffusely illuminated holographic recordings. Four experimental techniques were investigated to reduce the effect speckle imparted to the holograms of particulates resulting from the combustion process of solid metalized propellants in a two-dimensional rocket motor. The reconstructed holograms are used to provide data on the behavior of aluminum/aluminum oxide particles in a steady state combustion environment.

19. KEY WORDS (Continued)

retro-illumination
real image
particle field reconstruction
depth of field
rotating milar
absorption emulsion
transmission hologram
vibrating diffuser

20. ABSTRACT (Continued)

A 1 joule Q-switched pulsed ruby laser was used to illuminate Agfa-Gavaert 10E75 photographic plates. Reconstruction was done with a 1 watt beam from a Krypton laser. Results showed a 10μm improvement in resolution over non-assisted reconstruction techniques allowing discrimination of 11μm particles.

Approved for public release; distribution unlimited

Optimization of a Holographic Reconstruction Process for Combustion Phenomena

by

Marcus A. McInnis
Lieutenant, United States Navy
B.S., Maine Maritime Academy, 1975

Submitted in partial fulfillment of the requirements
for the degree of

MASTER OF SCIENCE IN AERONAUTICAL ENGINEERING

from the

NAVAL POSTGRADUATE SCHOOL
December 1982

ABSTRACT

This investigation addressed the resolution limiting speckle created in diffusely illuminated holographic recordings. Four experimental techniques were investigated to reduce the effect speckle imparted to the holograms of particulates resulting from the combustion process of solid metalized propellants in a two-dimensional rocket motor. The reconstructed holograms are used to provide data on the behavior of aluminum/aluminum oxide particles in a steady state combustion environment. A 1 joule Q-switched pulsed ruby laser was used to illuminate Agfa-Gevaert 10E75 photographic plates. Reconstruction was done with a 1 watt beam from a Krypton laser. Results showed a 10μm improvement in resolution over non-assisted reconstruction techniques allowing discrimination of 11μm particles.

TABLE OF CONTENTS

LIST OF FIGURES

LIST OF TABLES

I. INTRODUCTION

The development of high performance solid propellant rocket motors for use in modern weapon systems has led to an increased interest in the use of metal additives. Metals are especially attractive for space applications where the increased performance can be attained without the requirements for minimum smoke. These additives are employed in an attempt to increase the deliverable specific impulse of the rocket motors and to provide a stabilizing effect to potentially hazardous pressure oscillations within the combustor during combustion. Metalized propellants, however, are not without their problems. They are often difficult to vaporize and ignite, slow to burn, and may lead to the formation of high mass agglomerates. They also can reduce the percentage of complete combustion.

Many of the propellants currently use finely powered aluminum (1-50 microns). Particles of aluminum (Al) along with its oxides (e.g. Al_2O_3, AlO, and Al_2O) ranging in size from 0 to 30 microns exist, along with unburned metal (to several hundred microns) in the flow field of the rocket motor [Ref. 1]. These solid particles have a tendency to cause decreased exhaust flow velocity with the consequental reduction in thrust and specific impulse [Ref. 2] and are responsible for significant two-phase flow losses as the combustion gases expand through the nozzle. Fortunately, the gains from adding metals to solid rocket propellants more than balance the drawbacks where exhaust smoke can be tolerated.

For a more complete understanding of the interactions within metalized propellant combustion and for increased accuracy in performance predictions, theoretical propellant combustion models are being expanded. Such efforts should lead to further reduction of drawbacks and to increased practical realizations of the theoretical possibilities of metalized propellants. Validation of these models requires a substantial amount of accurate quantitative data.

To this end, attempts to collect the required data are underway. By relating metalized propellant properties and rocket motor operating conditions to the behavior of the particulates within the rocket engine and nozzle exhaust it is hoped that the current analysis and prediction models can be modified to appropriately reflect these variables.

Work at the Naval Postgraduate School has been directed at obtaining experimental data on the metallic particle sizes that exist (in the motor and exhaust nozzle at various operating pressures) within the gas phase. Four experimental techniques are currently being used to obtain and expand the knowledge in this area:

(1) High speed cinematography of burning propellant strands in a combustion bomb and of burning slabs within a two-dimensional motor with cross flow;

(2) Post fire residue collection and subsequent examination with a scanning electron microscope;

(3) Scattered laser power spectra measurements for the determination of mean particle diameters at the nozzle inlet and exhaust planes; and

(4) Holographic image construction of burning propellants in both strand and two-dimensional cross flow environments.

Diloreto [Ref. 3] conducted an initial investigation using high speed motion pictures and the scanning electron microscope techniques.

Karagounis [Ref. 4] refined the motion picture techniques and developed the initial holographic procedures for burning propellant strands and the initial techniques used for determining mean particle size at the nozzle exit from measurements of scattered light intensity.

Gillespie [Ref. 5] continued the development procedures to obtain holographic recordings of particulate behavior during the combustion process of solid propellants in a two-dimensional rocket motor.

Cramer and Hansen [Refs. 32 and 33] improved the techniques for determination of the volume-to-surface mean particle size using measurements of scattered light intensity and applied the method both at the entrance and exit planes of the exhaust nozzle.

The use of holographic techniques allows for the recording of phase information as well as the light amplitude (conventional photography). The inclusion of specific phase information of a coherent light source produces a three-dimensional recording of the reflected or transmitted light wave. Optimum utilization of this procedure can provide image resolutions to approximately three microns [Ref. 6].

The depth of field improvements over conventional photography are on the order of 100 times better; from .018mm for conventional photography to 1.8mm in a hologram for a 5 micron particle [Ref. 7]. In addition, flame and density gradient effects can be reduced and/or eliminated. A tradeoff between reduction in the recorded thermal gradients surrounding burning metal particles, and speckle creation, is however, necessary; as well as some sacrifice of depth of field to gain additional resolution

through lens assisted techniques [Ref. 8]. Obtaining particle size data from holograms is currently a very time consuming process. New methods in automated, computer-controlled optical processing are becoming available to obtain the data available in holographic recordings. These systems can significantly reduce the amount of time required over manually processing holograms of particle fields. They enjoy the advantage of being able to simultaneously break out particle size and field distributions at a variety of depths throughout the field in approximately one tenth the manual time. Algorithmic processing and new advances in electronic video signal and digital processing may some day surpass the advantage that manual reduction holds in particle discernability through mind/eye integration. Presently though, the major disadvantage in automated systems is the extremely large acquisition cost.

Manual reduction methods still offer a convenient means to analyze particle flow fields at a specific point and time. How ever the particle data in a hologram is obtained, improvement is still necessary in obtaining better resolution in the burning two-dimensional flow environment to allow for better accountability of the particles within the 2 to 10 micron range.

This investigation was directed toward gaining a better understanding of the variables affecting (creating) speckle and the techniques that could be used for reducing the amount of speckle during the reconstruction phase.

II. TECHNIQUES FOR RESOLUTION IMPROVEMENT

A. THEORY

1948 saw the introduction of a new concept of wavefront reconstruction by Dr. Dennis Gabor. Dr. Gabor attempted to create a means by which recorded electron waves could be reconstructed by the use of light. It had to, however, wait some twelve years before the problems he encountered with the lack of light's temporal and spatial coherence was overcome by the practical introduction of lasers. This two-step process of wavefront reconstruction, holography, uses a reference beam (in concert with the object wave (beam)) to establish a complex series of diffraction gratings.

Normal photography basically provides a method of recording the two-dimensional wave distribution of an image. The focused object waves' intensity is reacted to by the silver halide particles in the recording medium. All phase information created by the difference in traveling paths of the object wave (due to the objects depth) is lost.

In holography the phase information is retained by the inclusion of a reference wave created from the main wave (beam) before it impinges upon the object (see Figures 1 and 2). After the beam passes the object, both waves are directed onto a photographic plate (Figure 3). The unfocused waves create the diffraction pattern (grating) [Ref. 11] which stores both the phase and amplitude (intensity) information of the object wave. Temporal and spatial coherence must be maintained between the reference and objects waves [Refs. 9 and 10].

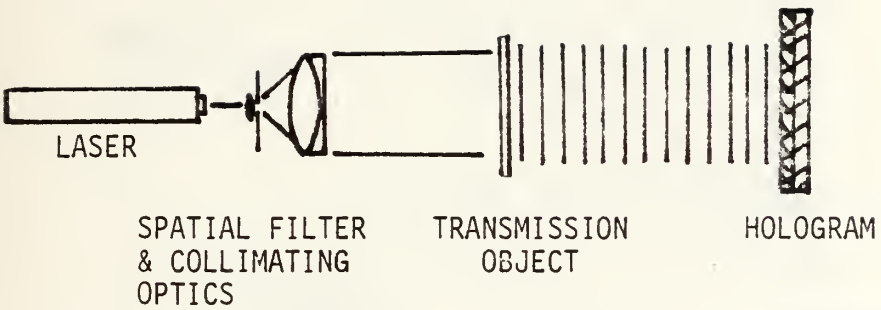

Figure 1. Inline Transmission Hologram

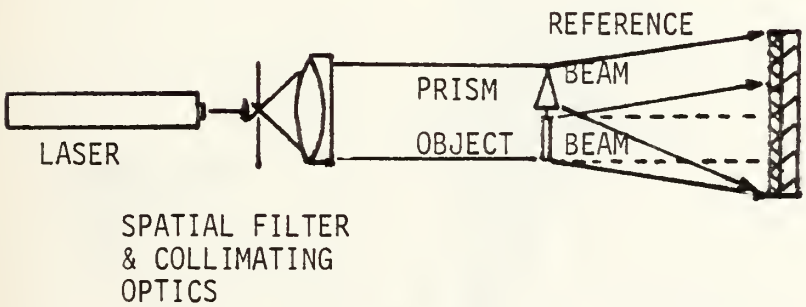

Figure 2. Off Axis Transmission Hologram

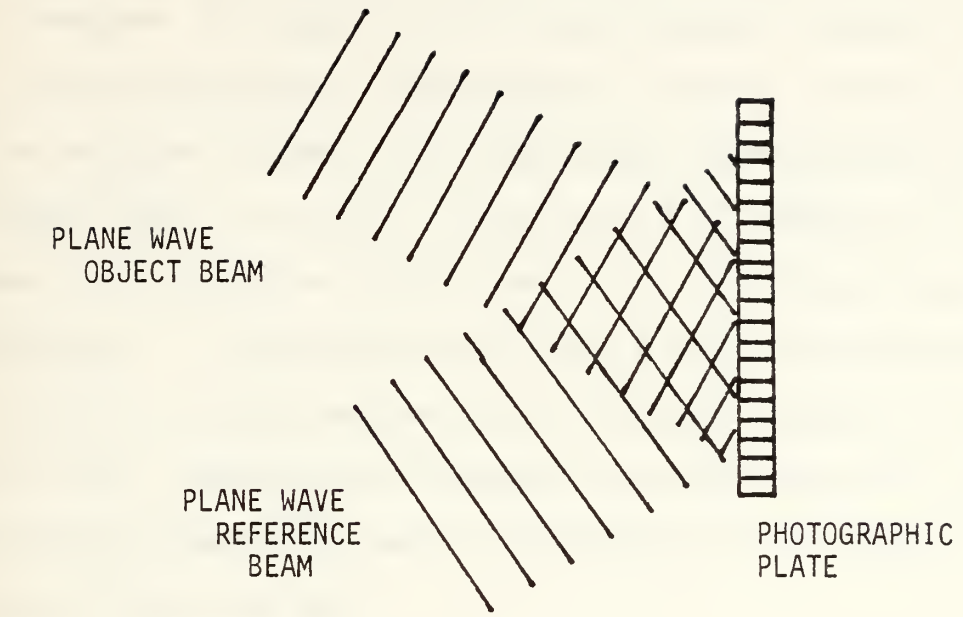

RECORDING THE TWO BEAM INTERFERENCE PATTERN

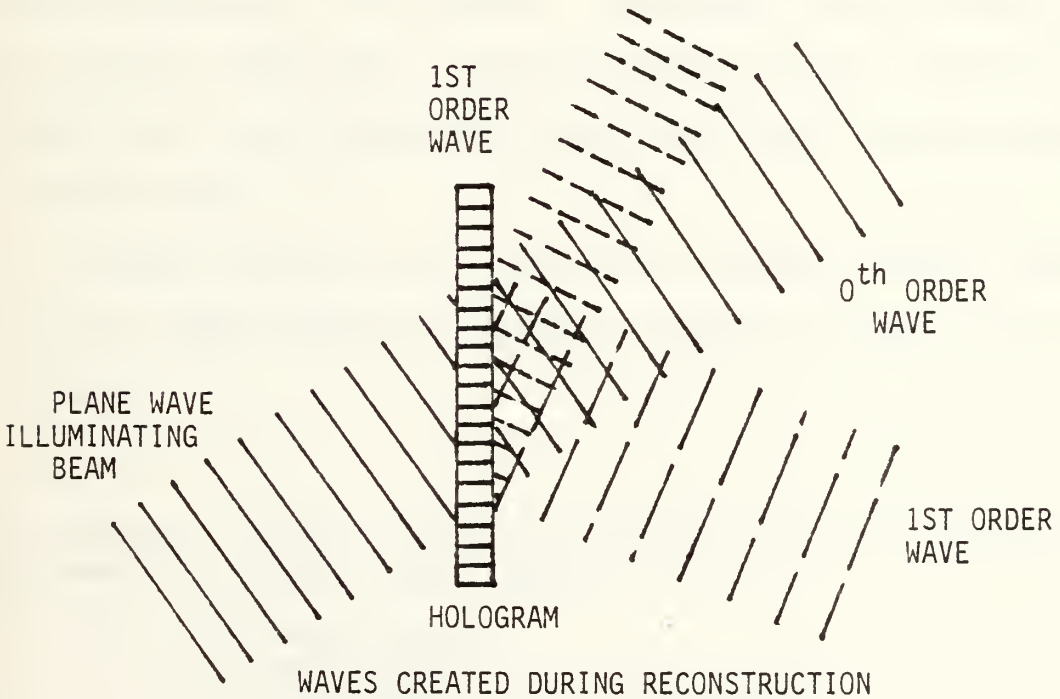

WAVES CREATED DURING RECONSTRUCTION

Figure 3. Plane Wave Hologram

There are two basic ways in which the diffraction gratings are stored, across the surface of the recording medium (plane holograms) and throughout the depth of the recording medium (volume holograms). In a volume hologram the fringe spacing is smaller than the dimensions of the emulsion so that the fringes become "stacked up" through the thickness [Refs. 12 and 13]. Fringe spacing is dependent on the angle between the reference and object beams and the recording light frequency[1] ($d=\lambda/2\sin\frac{1}{2}\theta$). If this angle is at least 7° or 8°, and the recording is made from the visible spectrum, the diffraction grating will be on the order of 2μ. Most emulsion thicknesses are 5-20μ [Ref. 31] (Table 1), therefore most recordings made on photographic film or plates are considered of the volume type.

It is the density of these diffraction gratings that make recording on normal photographic film useless. Conventional film has the capability to record between 200 to 400 lines per millimeter. Holographic recordings require up to 2000-3000 lines per millimeter to be effective [Ref. 17] (see Table 2).

In viewing a hologram the reconstruction provides several images. The two main images produced are normally referred to as the "real" and the "virtual".

---

[1]The formula is known as the Bragg condition for the constructive interference of diffracted light. Where:

d = fringe spacing
λ = wave length
θ = angle between the two wave fronts

Table 1. Approximate Thickness and Intensity Transmittances of Selected Silver Halide Emulsions [Ref. 31]

EMULSION	THICKNESS (μm)	INTENSITY TRANSMITTANCE 6328Å	5145Å	4880Å
649F Plate	15	0.42	0.40	0.33
649F Film	6	0.81	0.61	0.62
High Res. Plate	6	0.81	0.58	0.58
10E56	6	0.67	0.35	0.29
10E70	6	0.47	0.37	0.29
10E75	6	0.61	0.50	0.40

Table 2. Manufacturer-Specified Resolutions of Selected Silver Halide Photographic Emulsions

RESOLUTION (lines/mm)	EMULSION
1500	14C70, 10C75
Over 2000	649F, 649GH, HRP
2800	10E56, 10E70, 10E75
3000	8E56, 8E70, 8E75

(Adapted from Ref. 15)

The diffraction gratings stored in the photographic medium exhibit lens-like properties and provides a means of generating either the reference beam wave front or the object beam wave front. If the stored diffraction grating (photographic plate) is illuminated by the reference wave from its original direction, it will generate the object wave, producing the object image in its original position and orientation when viewed from behind the plate (Figure 4). This is termed the virtual image[2]. It exists as if the object were still three-dimensionally present. Other images are also produced, Zeroth, first and second order diffractions, with the higher ordered diffractions much weaker and usually not considered [Ref. 15]. The other major image produced from this reconstruction will be a geometrically distorted real image on the same side of the plate as the viewer (in this example). This focusable image can be seen by placing the eye or a piece of paper at the proper point. It is the real image that can be of most use in trying to record the reconstructed holographic image. By using a conjugate reference beam (retro-reflected) (Figure 5), a distortion free real image will be pseudoscopically[3] produced.

Undesirable features of the holographic technique may include a variety of optical aberrations, near to far field distortions, speckle, and noise originating from the optical components and development

---

[2]A virtual image is formed if the distance between the lens and an object is less than the focal length. It is called virtual since it is not physically located anywhere, it only appears to be [Ref. 14, p.316].

[3]Pseudoscopic, opposite of orthoscopic, meaning inverted depth, turned inside out and back side too at the same time [Ref. 16].

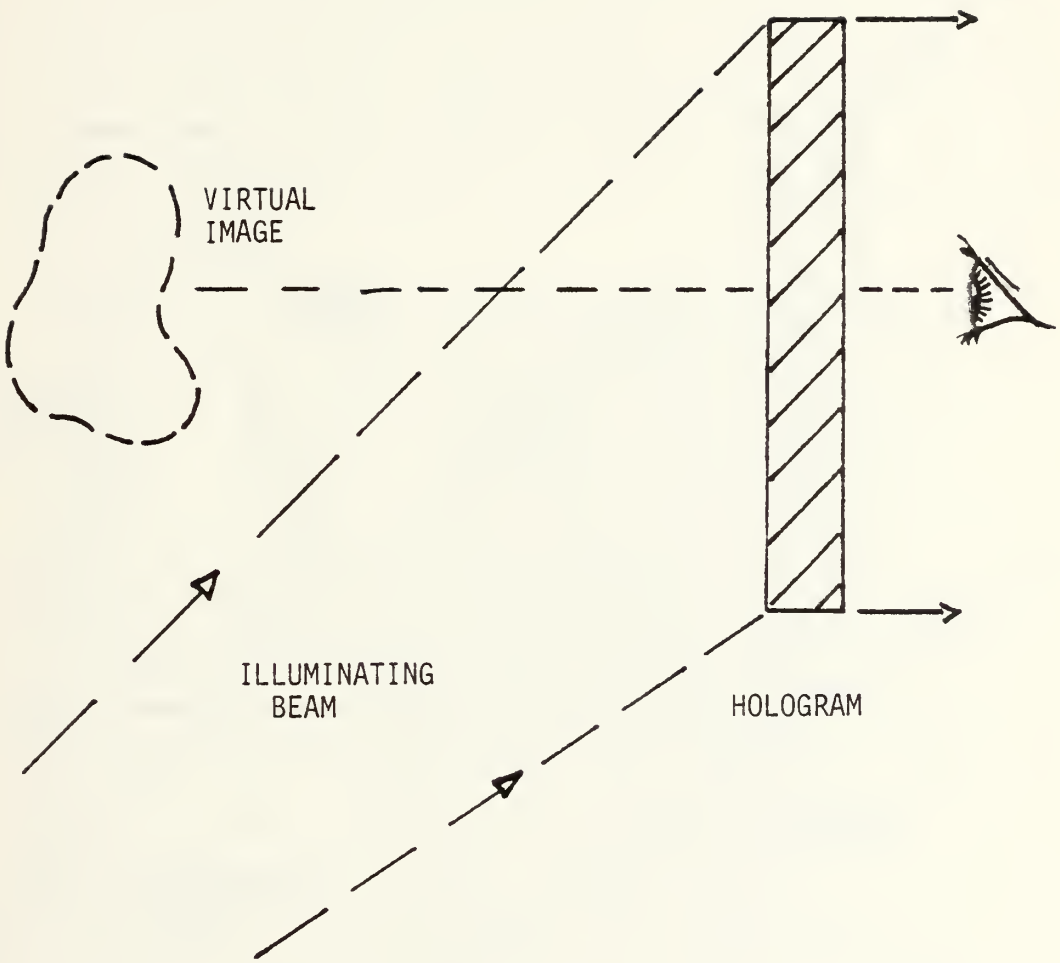

Figure 4. Virtual Image Generation

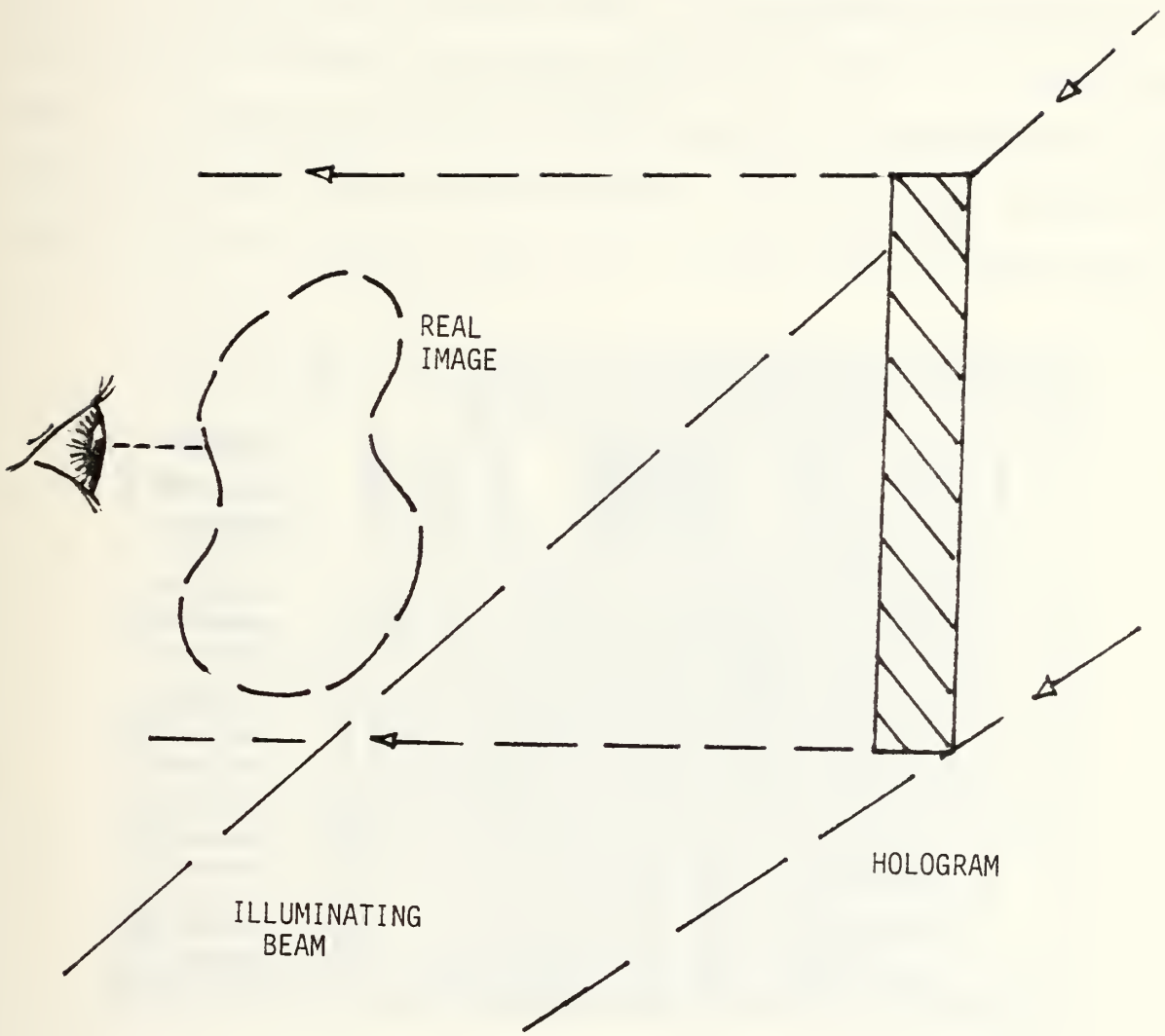

Figure 5. Orthoscopic Real Image

process. A more complete understanding of these may be gained from Collier and Smith [Refs. 18 and 19]. This investigation concentrated on the effects that speckle introduces to resolution because of the required diffuse illumination of the particles in the combustion process.

B. TAKING THE HOLOGRAM

Application was made of the techniques developed by Karagounis [Ref. 2] as modified by Gillespie [Ref. 1] for recording the behavior of particulates produced from burning propellant strands in a combustion bomb. To produce an initial resolution base for this investigation, the combustion bomb set-up outlined in Ref. 1 was replaced by a 1951 Air Force resolution target (Figure 6). A lens assisted .6943 micron,

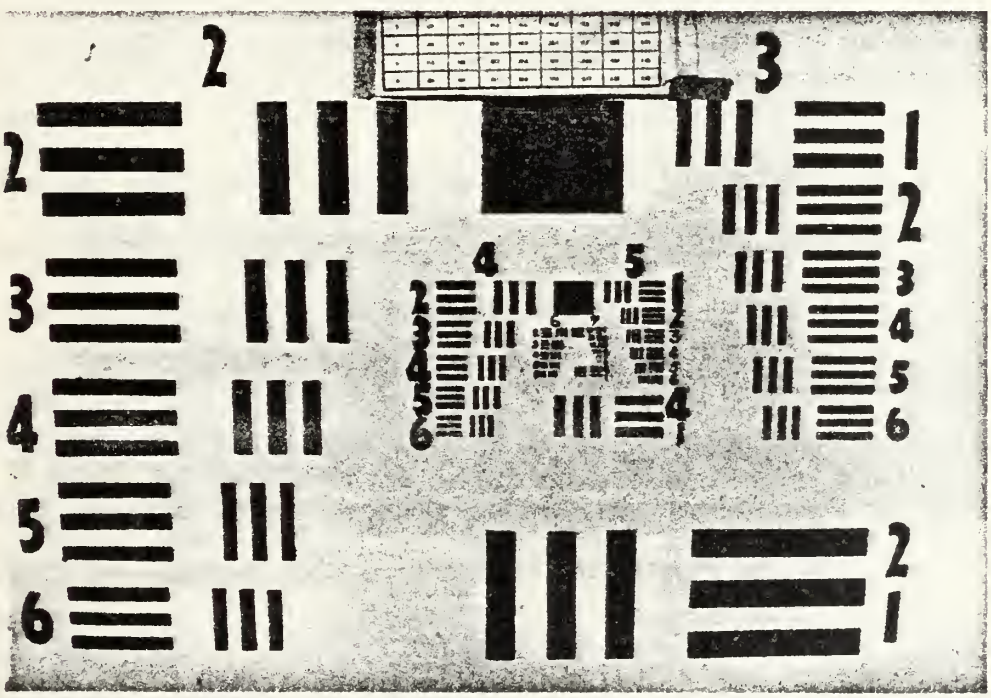

Figure 6. 1951 Air Force Resolution Target

pulsed ruby laser system (as described in Refs. 20 and 21 and shown in Figures 7 and 8) was used to record the holograms, schematically shown in Figure 9. This holographic system was used to produce transmission holograms using an absorption medium. The reconstructed image used was the projected orthoscopic real image, produced by retro-illuminating the hologram at the same reference angle.

The Q-switch pulsed ruby illuminator is capable of producing pulses of 50 or 10 nanosecs, with one or 0.25 joules of power respectively. These pulse durations are necessary if blurring of the moving particles is to be eliminated [Ref. 22]. Diffuse illumination of the object was used because it reduced the blooming and thermal (gradient) effects caused by the burning particles. This had the disadvantage of introducing speckle onto the hologram. It also limited the useful effects gained by using the aperture increasing assisting lens coupled to the holocamera (Figure 10) when the reconstructing wavelength was different than the one used for illumination [Ref. 23]. These lenses also fixed the speckle size introduced and further reduced the depth of field[4]. A discussion of the results obtained with diffuse and collimated illumination and the use of lens assisted holocameras is contained in Ref. 24.

A five/four to one reference beam to object beam intensity ratio was maintained by the proper use of neutral density filters. The filters were added or removed as a function of the amount of smoke and particle

---

[4]The depth of field was already limited by forming the hologram by the transmission method.

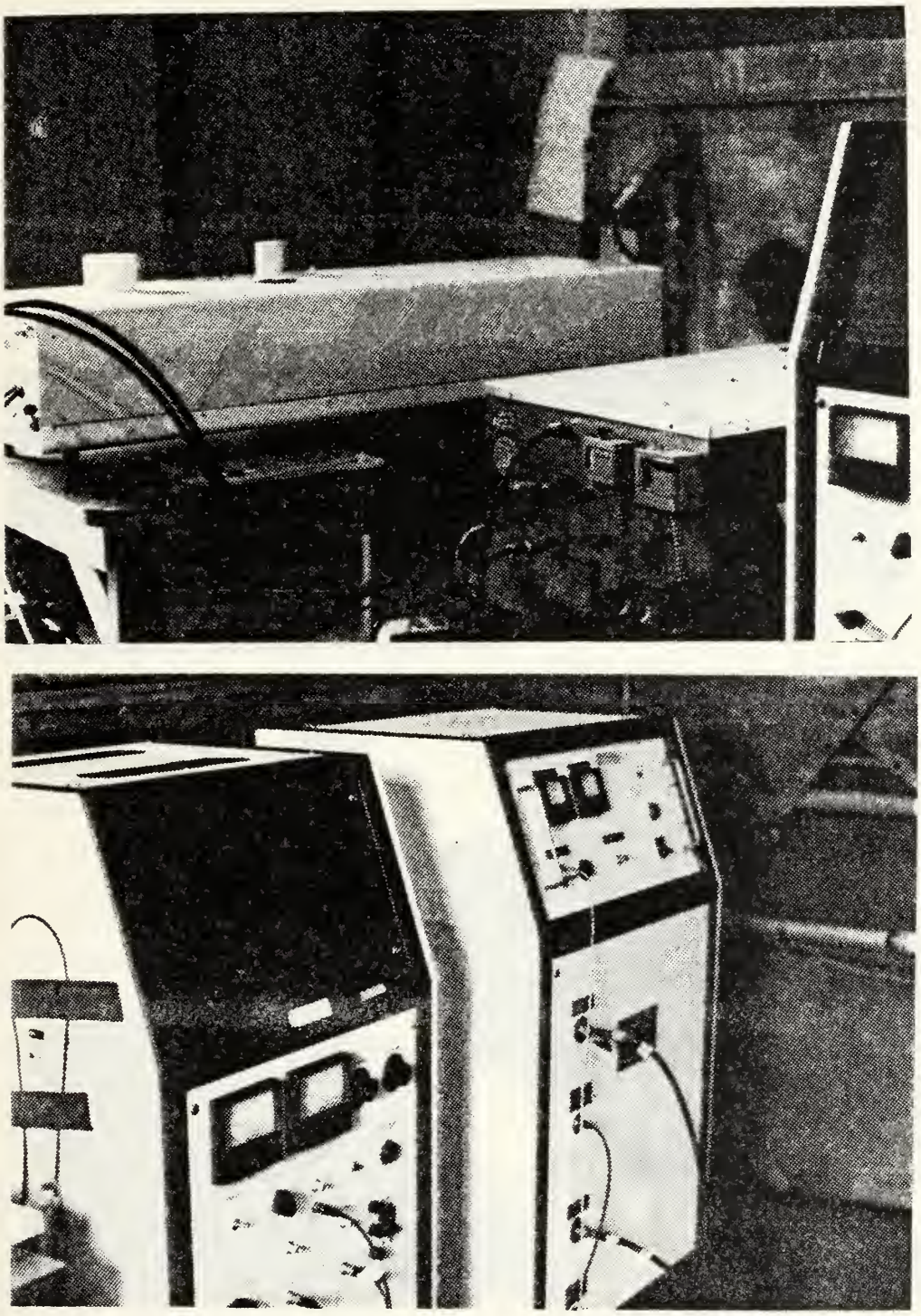

Figure 7. Pulse Ruby Laser

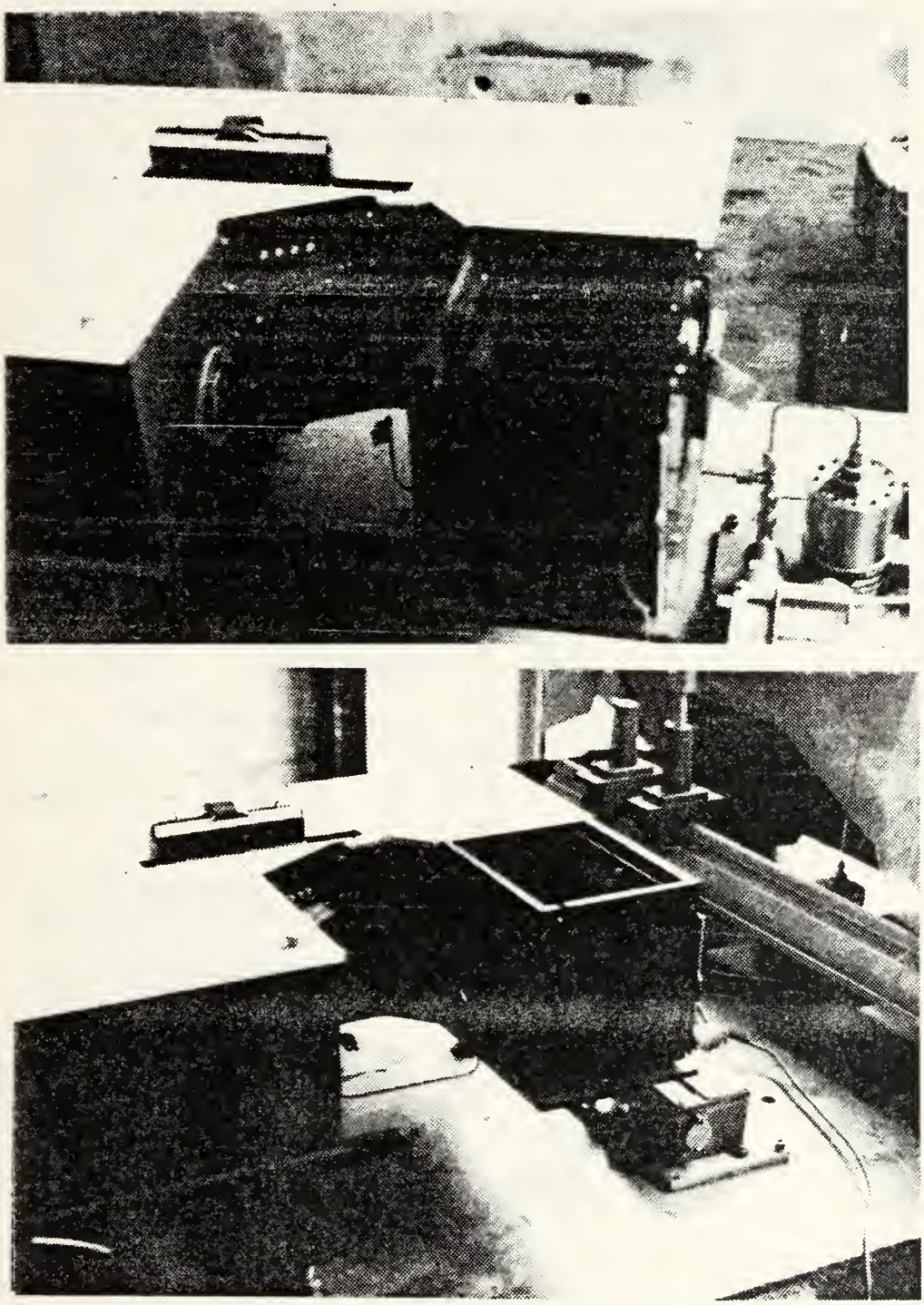

Figure 8. Holocamera Set-Up

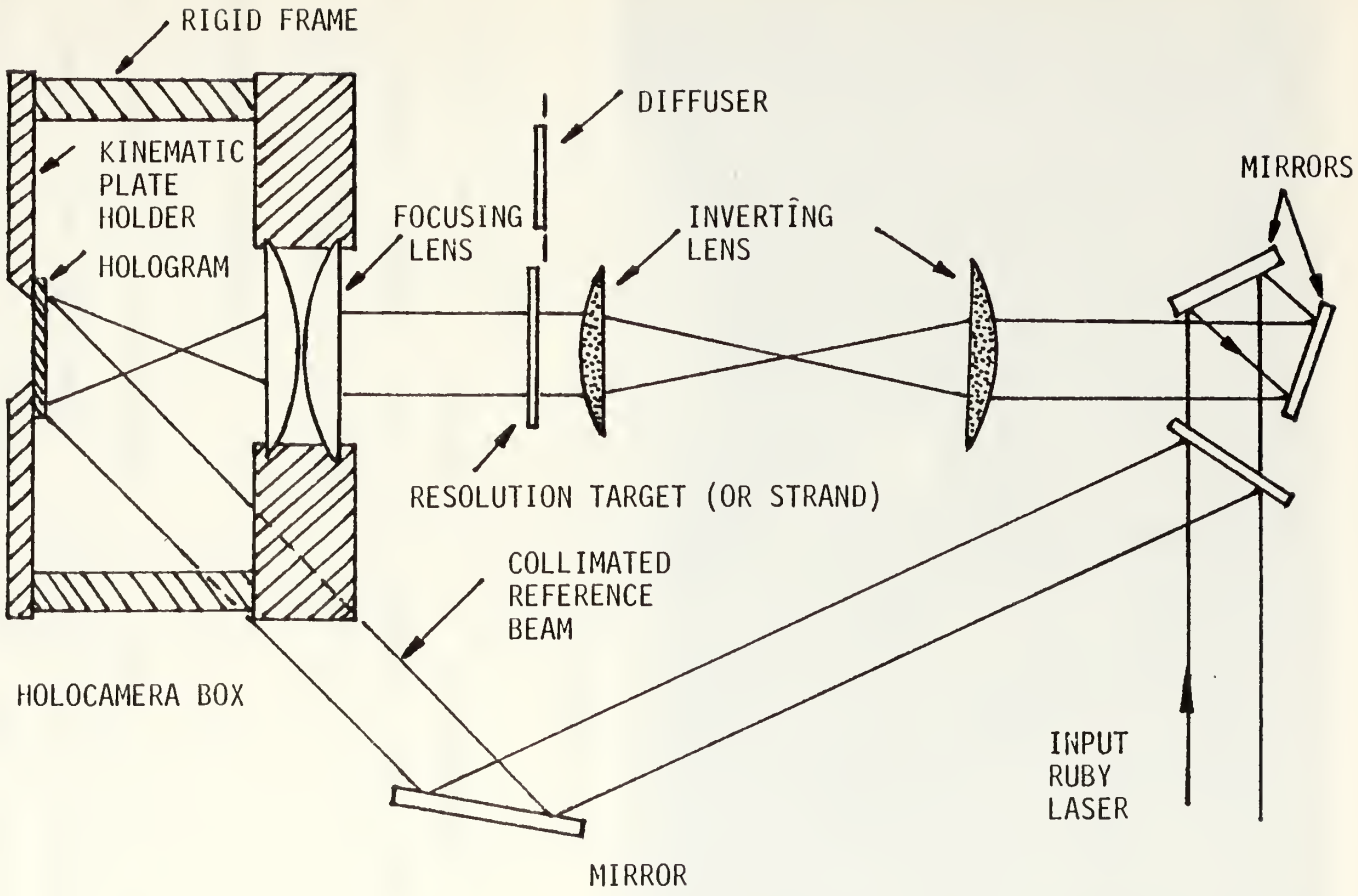

Figure 9. Schematic of Lens Assisted Holographic Arrangement (Adapted from Ref. 4)

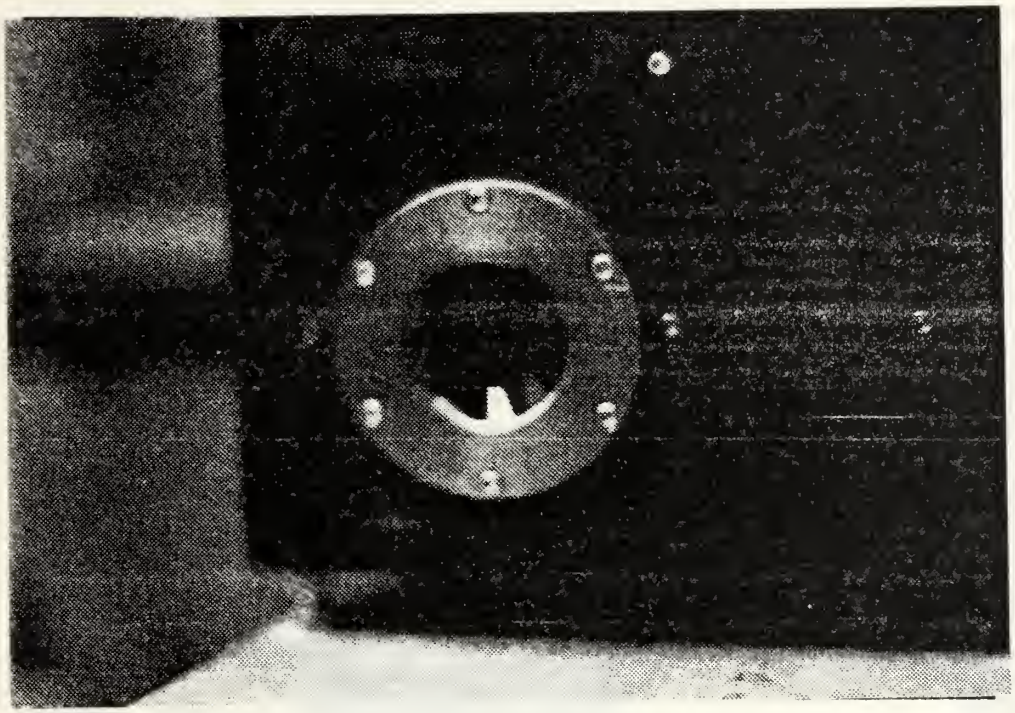

Figure 10. Assisting Lens on Holocamera Box

density expected during the exposure, based on experience. For the resolution target hologram, filters were added in the reference beam path. The firing sequence is presented in Ref. 27.

C. PROCESSING THE HOLOGRAM

After the exposure the holocamera box (Figure 11) was removed[5] to the darkroom for plate development. Agfa-Gevaert 10E75 absorption type photographic plates were used because of their sensitivity to the ruby

---

[5]One of the designed advantages of this particular holocamera system is that the plate rested in the same holder for illumination and reconstruction.

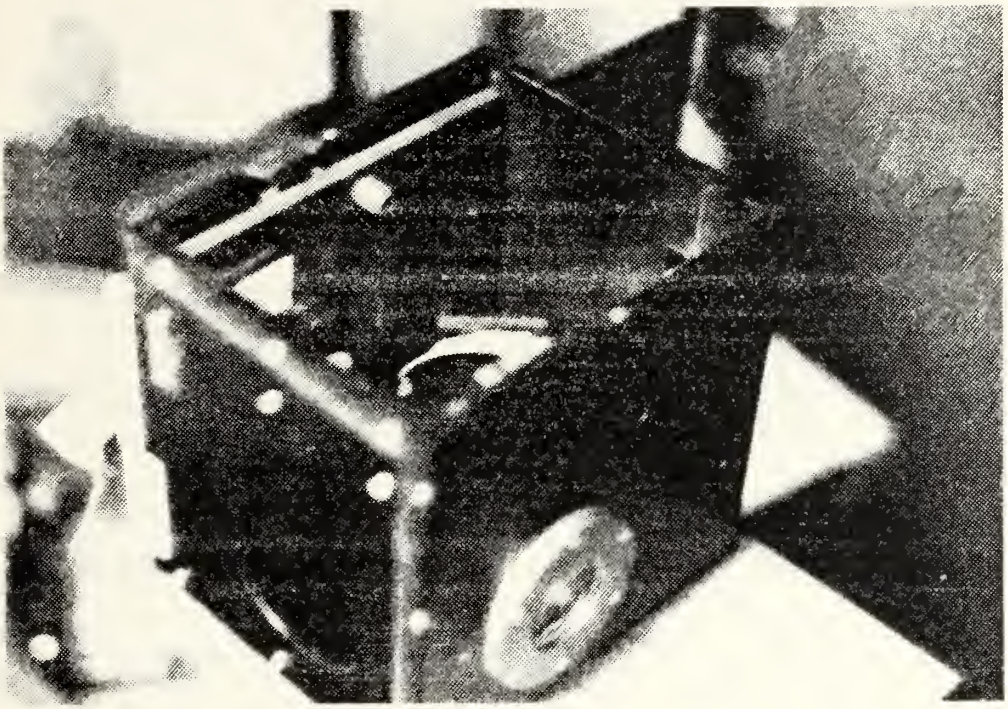

Figure 11. Holocamera Box

laser wavelength (Figure 12) and excellent resolution properties (Table 2).

In the darkroom the plate was removed for normal development procedures, which are shown in Table 3.

Alternate development techniques are given in Ref. 14[6].

---

[6]As mentioned earlier, the development process can be a significant contributor of noise in the final product. This investigation was concerned with speckle suppression so this area was not addressed. However, improvements in the ultimate particle resolution are possible and recommendations for those improvements are made in the applicable section of this report.

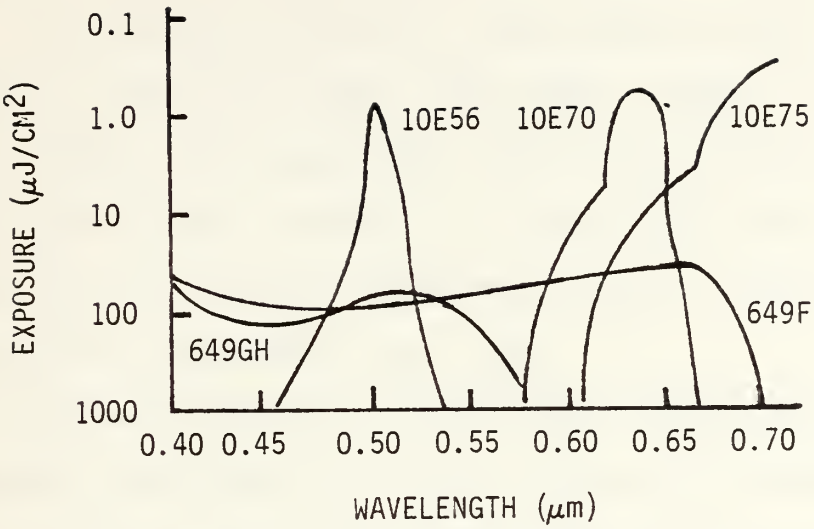

Figure 12. Spectral Sensitivity Curves for Photographic Emulsions

Table 3. Development Process for Absorption Holograms

(1) Develop using Kodak D-19 processing agent, quarter strength solution as suggested, 1-3 mins, inspecting periodically under safelight for a 50-70% dense image.
(2) 30 sec. in Kodak stop bath.
(3) Fresh water rinse.
(4) 5 to 7 min. Kodak Rapid fixer.
(5) 10 to 15 min. rinse in fresh water.
(6) 30 sec. in Kodak "Photo Flo" solution.
(7) Air drying.

D. RECONSTRUCTION LASER

The laser used in reconstruction was a Spectra-Physics Krypton model 165-11. The vertically polarized 1.25mm beam was capable of producing 1.6 watts at the .6471 primary line used, although it was rated for operation under 1 watt beam power. The laser head was powered by the model 265 exciter and connected by an eight foot umbilical. Desired line selection was adjusted on the laser head with the aid of a single color operation prism assembly [Ref. 28].

The beam passed through a Spectra-Physics' model 332 spatial filter and expanding lens assembly which was coupled with the model 336 collimating lens telescope [Ref. 29]. The reconstruction beam was positioned at the reference beam angle and directed into the holocamera box by physically positioning the laser head unit.

E. SPECKLE SUPPRESSION METHODS

By selecting to diffusely illuminate the object volume the thermal effects were optically minimized[7], however; this diffuse illumination introduced a pnenomenon known as speckle. A conventional light source will not (to any great degree) interfere with itself or with other light sources because of its general lack of temporal and spatial coherence. Laser light also lacks the ability to constructively add (or destructively add) to another laser source if this coherence is absent. But,

---

[7]Diffuse illumination also allows each effective scattering center created to be recorded throughout the overall hologram [Ref. 15, Chapter 8.2].

when laser beams displaying coherence are selectively or mutually mixed, there will be constructive and destructive interference generated over the spatial coherent portions of the beams at that point of mixing.

This pnenomenon is readily apparent anytime laser light is reflected off most surfaces. The microscopic roughness of the surface will act as scattering centers, scattering portions of the reflected beam (inducing random phase changes) such that the mutual interference taking place will be evident in the apparent scintillation at the point of reflection.

The grain size of the speckle pattern depends on the smallest aperture of the recording or viewing instrument and on the distance of the observed surface [Ref. 30]. Any change in aperture size, distance, or change in viewing angle will perceptibly alter the interaction of the various wave amplitude additions and subtractions, changing the speckle pattern.

The first four experimental techniques examined in this investigation addressed the already existing speckle pattern evident in a diffusely illuminated exposed hologram. The fifth set-up was an attempt to reduce the amount of speckle recorded in the hologram.

1. Effects of Film Type and Recording Magnification

Initially, a variety of photographic films were tried and compared for resolution using the microscope and camera set-up depicted schematically in Figure 13 and pictured in Figure 14. The camera was coupled to the microscope using a standard microscope adapter. Beam power levels were recorded along with laser head aperture size for different exposure times for the various ASA ratings of the different films. Focusing adjustments were necessary when the camera was added

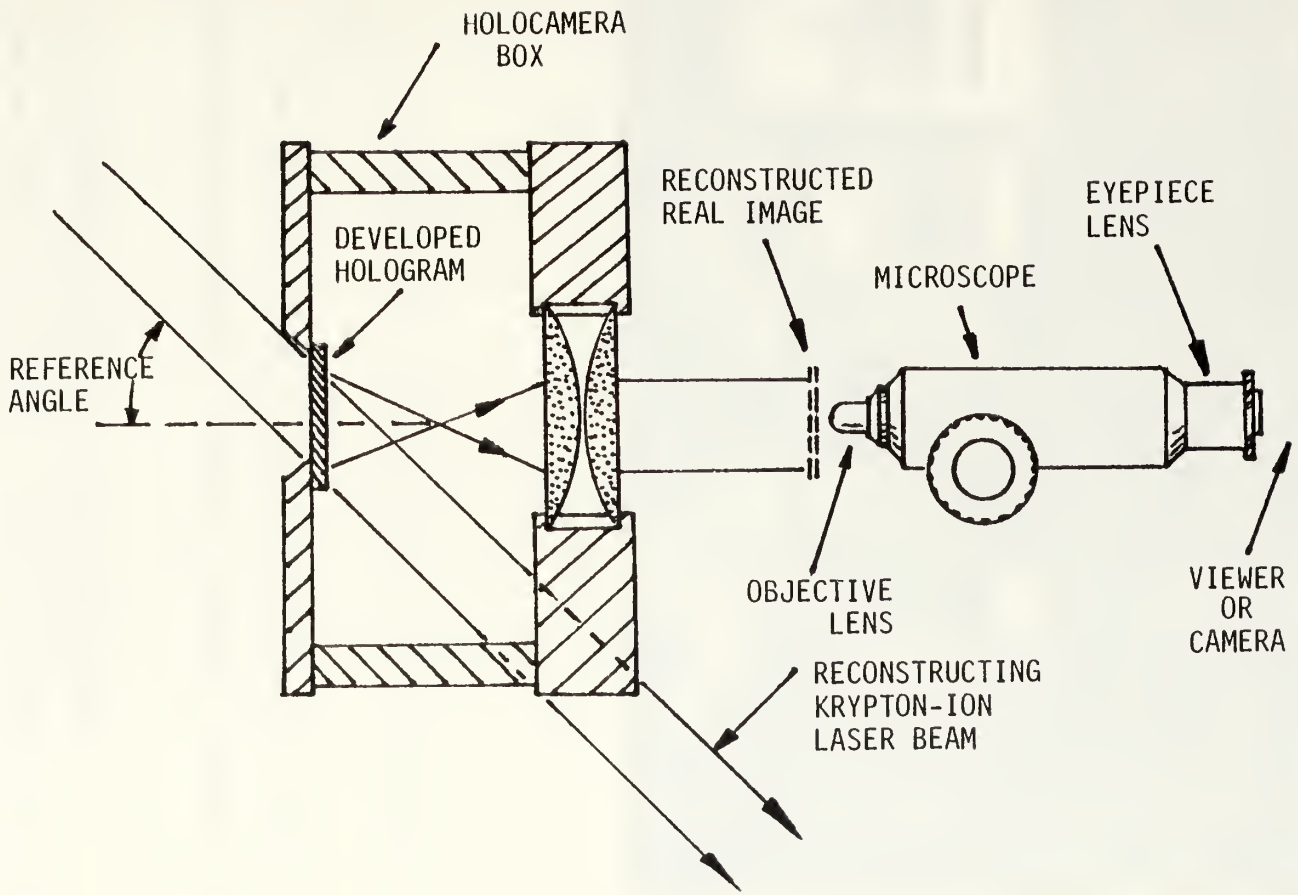

Figure 13. Schematic of Holocamera Box and Microscope
(Adapted from Ref. 4)

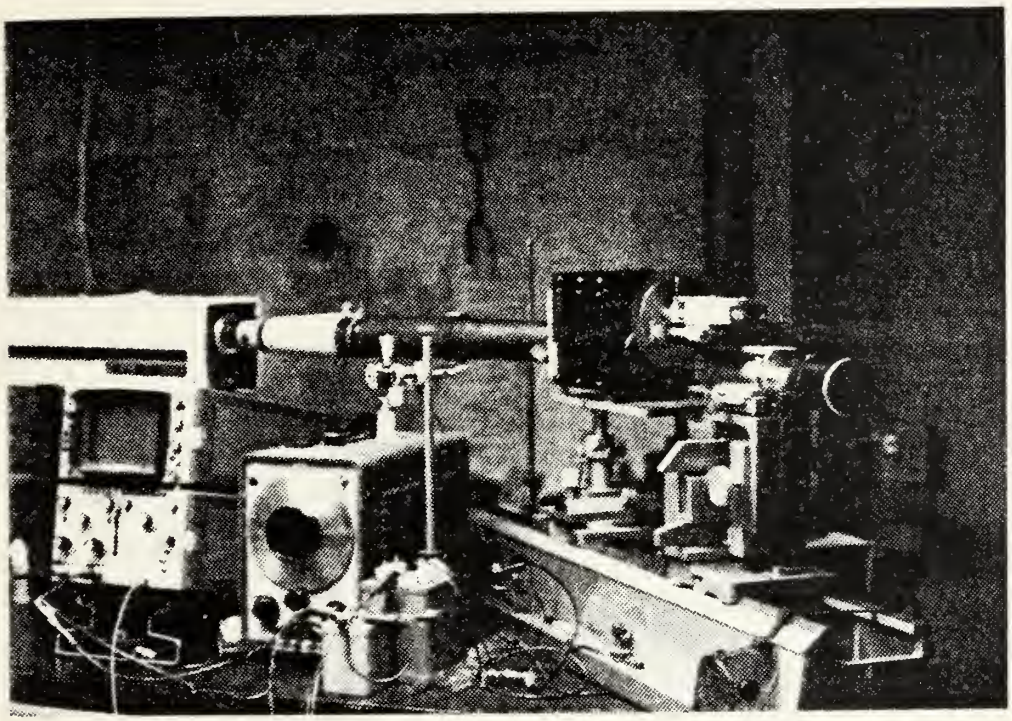

Figure 14. Holocamera Box and Microscope

after the initial sighting was set-up without it. Films used are presented in Table 4.

Next, the objective and eyepiece lens powers were varied to determine magnification effects on speckle size and ultimate resolution (Table 5).

2. Use of a Rotating Milar Disk in the Viewing Path

A rotating milar disk (Figure 15) was used [Ref. 23] as modified by Gillespie [Ref. 1]. The disk was located at the focal length of the objective lens of the microscope using a micrometer translation stage located above, and fixed to the microscope. The entire reconstructed

Table 4. Selected Photographic Films

	MANUFACTURER	FILM DESIGNATION	TYPE OF PROCESSING	ASA
1	Kodak	Panatomic X	B/W Prints	32
2	Kodak	Plus X Pan	B/W Prints	125
3	Kodak	Kodacolor II	Color Prints	100
4	Fuji	Fuji Color II	Color Prints	100
5	Kodak	Kodachrome 25	Color Slides	25
6	Kodak	Ektachrome 64	Color Slides	64
7	Kodak	Kodachrome 64	Color Slides	64
8	Kodak	Ektachrome	Color Slides	400
9	Fuji	Fuji Color 400	Color Slides	400
10	Kodak	Rapid Process Copy	Prints	Approx 1

Table 5. Selected Objective and Eyepiece Lenses

TYPE/MANUFACTURER	SPECIFICATIONS	USE
#80.3015 Achromat	1:1/60 FL	Objective
#80.302 Achromat	2:1/46.8 FL	Objective
#80.3515 Achromat	5:1/32 FL	Objective
Bausch & Lomb	10:1/16 FL	Objective
Leitz	UM 10:1/0.22	Objective (variable apperture)
Bausch & Lomb	5x	Eyepiece
Ramsoen	10x → 20x	Eyepiece
#80.0350	10x	Eyepiece

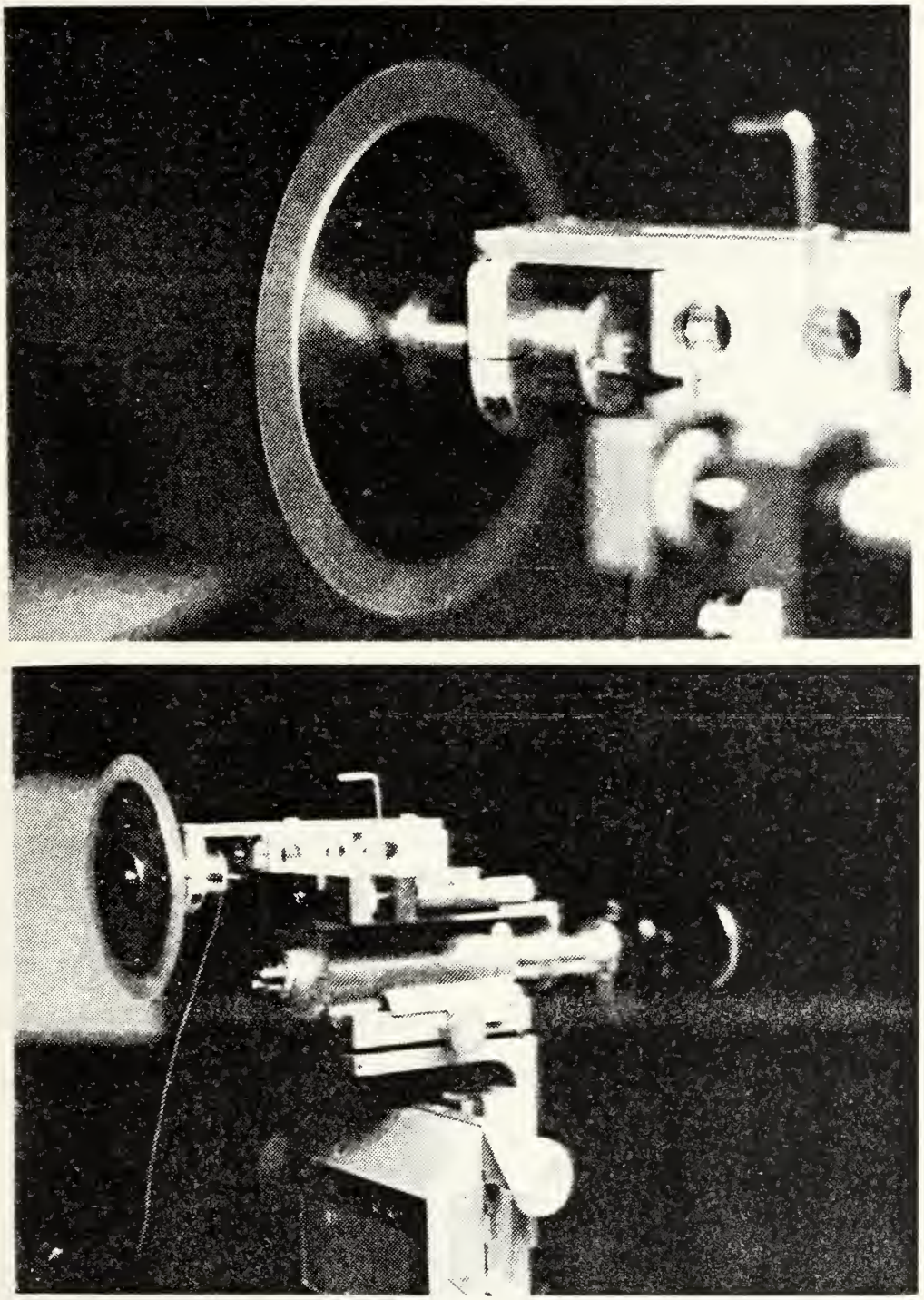

Figure 15. Milar Disk

"real" image provided from the holocamera box could be observed by X-Y-Z positioning of the microscope. The milar motion[8] was used to superficially time average the varing intensities inhertent in the speckle field, as seen by the eye.

3. Variation of Viewing Aperture During Recording Process

A "Leitz" UM 10:1/0.22 objective lens (Figure 16) with an internally variable aperture was placed in the microscope. The eyepiece lens magnification was 5x. Timed exposures were taken at selected power settings while the aperture was varied at different rates throughout the exposure period. Additional runs were made using the same method but also employing the rotating milar disk.

4. Use of a Linear Motion Diffuser in the Viewing Path

A vibrating diffuser (Figure 17) was constructed and positioned at the focal point of the microscope objective lens. This was an attempt to use the rectilinear motion of the vibrating diffuser in substitution for the rotary motion of the rotating milar disk. Slight axial movement by the rotating milar coupled with the earlier discussed reduced depth of field of the reconstructed image posed focusing problems that could effect particle resolutions. Restricting the motion of the diffuser along the focal plane was designed to enhance the speckle averaging while reducing the effects of warping and misalignments of the milar disk.

---

[8]Any motion causing the scattering centers to change at a rate approaching 100 HZ will exceed the eyes ability to discern the individual motion.

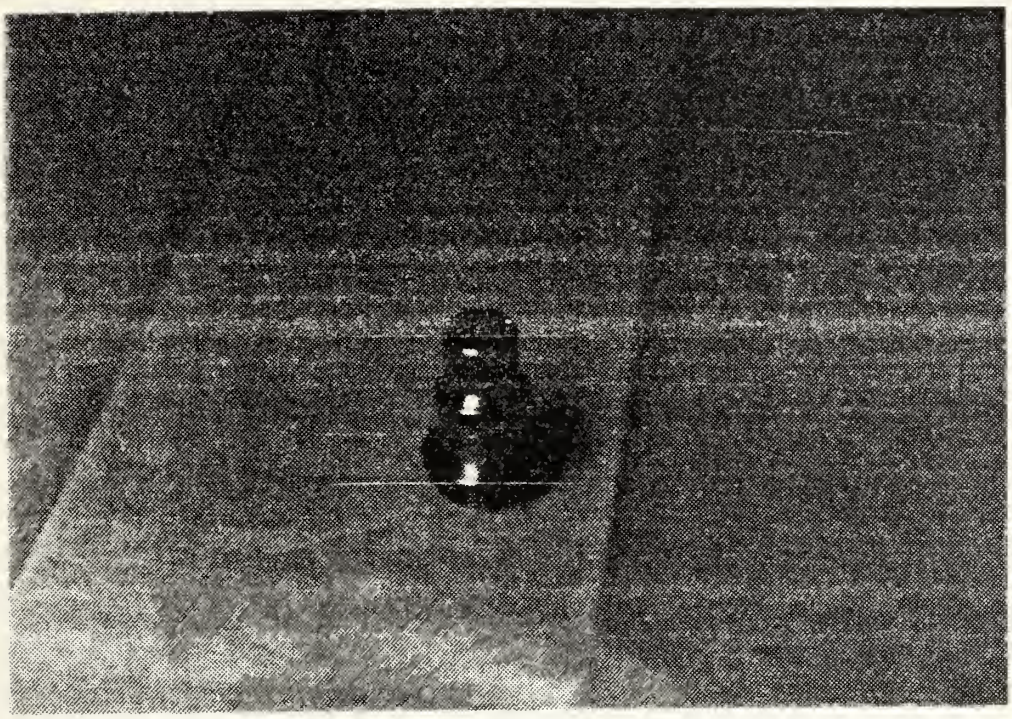

Figure 16. Leitz 10x Variable Aperture Objective Lens

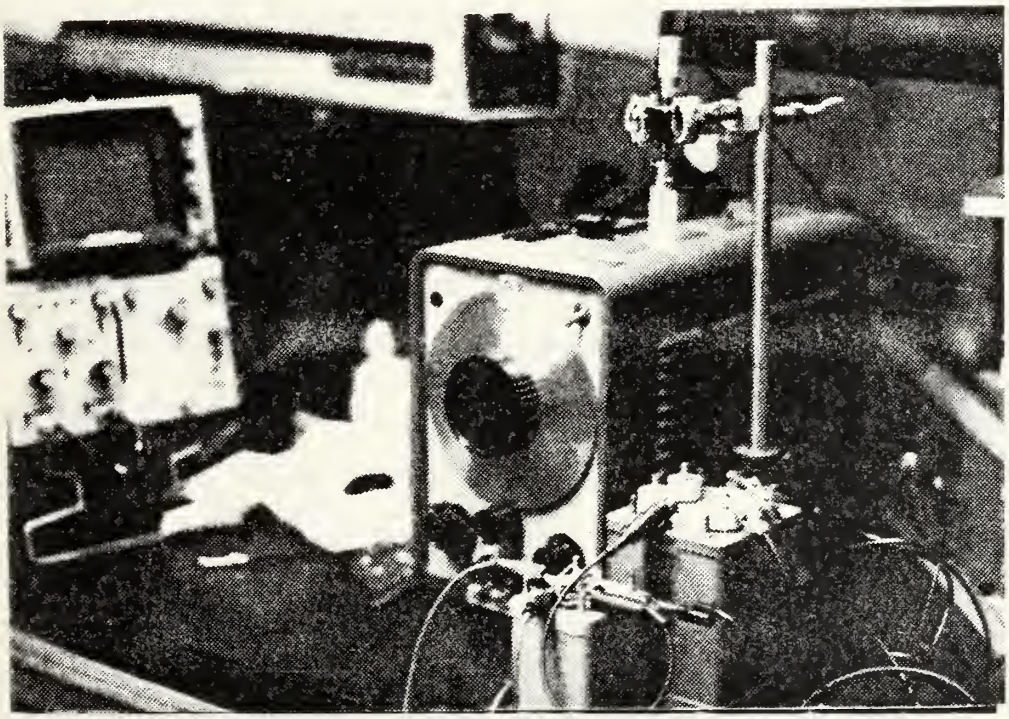

Figure 17. Vibrating Diffuser Set-Up

The vibrating diffuser consisted of:

(1) a single strength ground glass diffusing plate, 2 x 3 inches;

(2) a DC piezoelectric crystal micro-positioner;

(3) a Hewlett Packard model 200CD wide range oscillator, and

(4) a variable tap Raytheon transformer.

The signal generator provided a 25 volt (at 42 mA) ac signal set at 200 HZ[9] to the transformer, where the signal was boosted to 460-633 volts (at 1.9 to .42 mA, respectively). The micropositioner was rated up to 1000 volts (at 2 milliamps).

The vibrating diffuser was attached to the traveling vernier above the microscope and positioned in the same manner as the milar disk. Two types of diffusing patterns were used. A single strength piece of ground (sand blasted) glass and a piece of opal glass. An alternate method of placing the micropositioner on a seperate (free standing) holder was used to isolate unwanted vibrations to the microscope.

5. Use of Moving Diffusers in the Hologram Recording Process

The last technique tried was an attempt to improve the resolution of the hologram by reducing the amount of speckle recorded. An eight-inch diameter ground glass disk was attached to an unloaded series wound motor. The disk (and motor) was positionable through support adjustments (Figure 18) so that it could be located in front of the ruby laser illuminating window. The usual diffuser was removed and the

---

[9]200 HZ was an arbitrary figure chosen to ensure at least a 100 HZ rate and to provide adequate frequency for electrical equipment.

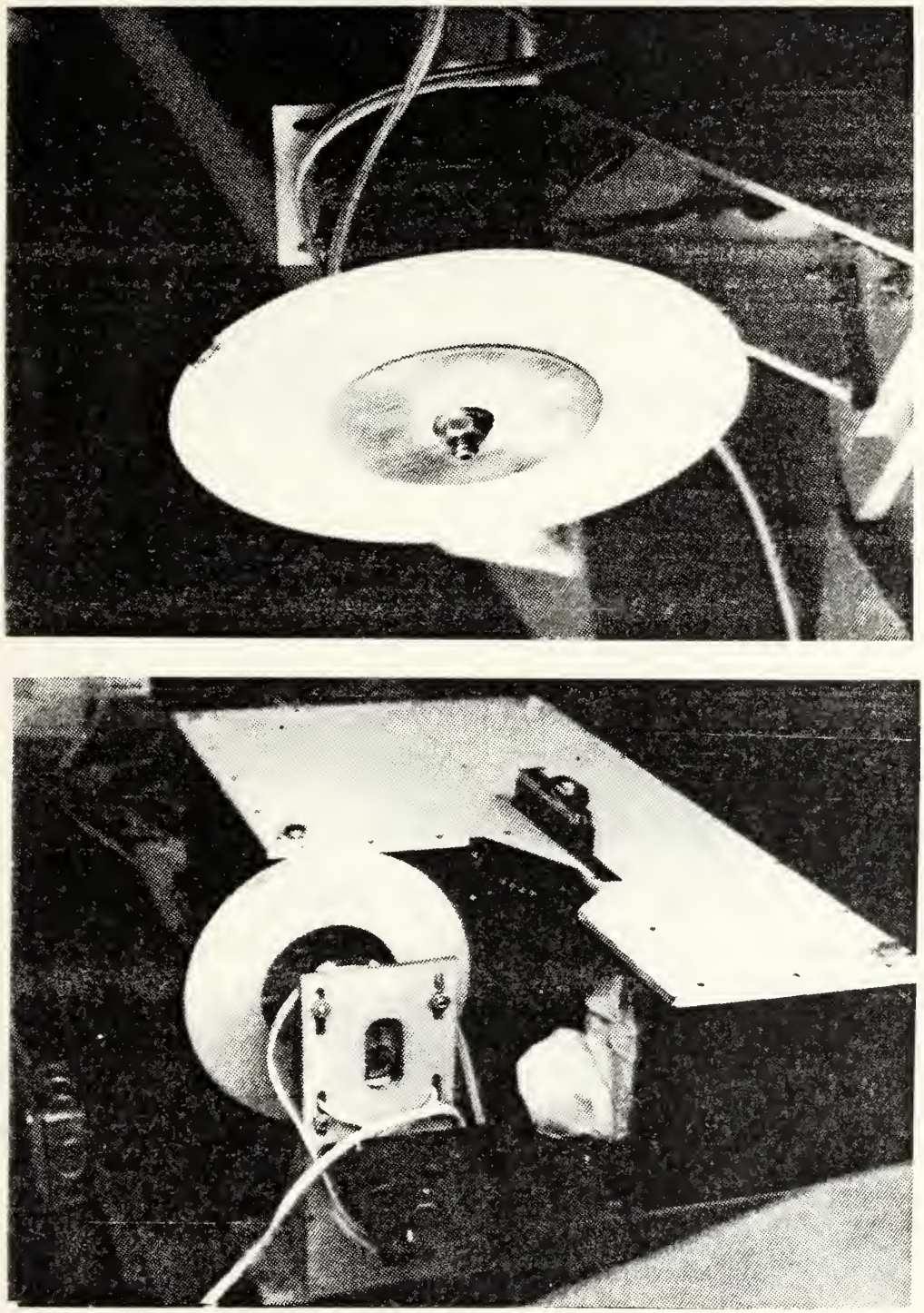

Figure 18. Rotating Illuminating Beam Disk

diffusing disk positioned so that the object beam passed through it on the way to the resolution target and holographic plate.

The size of the disk was dependent on the motor used which was a function of the rotational speed required to produce the effective motion during the pulse duration of the ruby laser. The radial distance a point on the disk travels was found by:

$$D = \omega r t$$

where

ω = rad/sec
r = radius (meters)
t = time duration of the laser pulse

For example,

$$D = (3000 \frac{rev}{min}) 2\pi \frac{rad}{rev} (4 \text{ in}) \frac{.0254m}{in} (50 \times 10^{-9}) \text{ sec } \frac{1 \text{ min}}{60 \text{ sec}}$$

$$= 1.6 \text{ microns}$$

Thus, at 3000 rpm the range of distances that would pass before the illumination beam (.6943 micron wavelength) was from .8 microns on the inside diameter to 1.6 microns on the disk edge. Again, two diffusion patterns (granular densities) were used, ground and opal glass. The speed of the motor was controlled through a precalibrated rheostat and optical cycle counter.

III. RESULTS AND DISCUSSION

To record the information present in the hologram, the real image created by retro-illuminating the recorded hologram with a collimated .6471μm Krypton laser beam was positioned (projected) to the objective lens of the microscope. A Cannon AE1, 35mm single reflex camera was attached rigidly via a microscope adapter.

1. Films and Lenses

An accurate reduction of the data stored in the hologram required that the photographic film used possess minimum grain and appropriate frequency sensitivity. Several film types were used (Table 4). Good results were obtained using both black and white (B&W) prints and color slides. Of the B&W films Panatomic X gave the best results, allowing resolutions of 11μm when used with a 1:1 objective lens, 5x eyepiece, and the rotating milar disk (Figure 19). The color print films (any ASA rating) could not equal the resolution capability of the B&W print films. The best color slide film (Kodachrome 25) produced 11μm resolutions (Figure 20) at magnification of 5x to 20x, surpassing Panatomic X at higher magnifications (Figure 21). The slower speed films, 32 ASA for Panatomic X and 25 ASA for Kodachrome 25, surpassed other films in final resolution capability overall. Speckle size in the higher magnifications became a problem. The grain size of the film can help reduce this effect a little. Shown in Figures 22 and 23 are two 20x exposures of the same hologram. Figure 22 is Ektachrome 400 while Figure 23 is Kodachrome 25. The larger film grain of Ektachrome 400

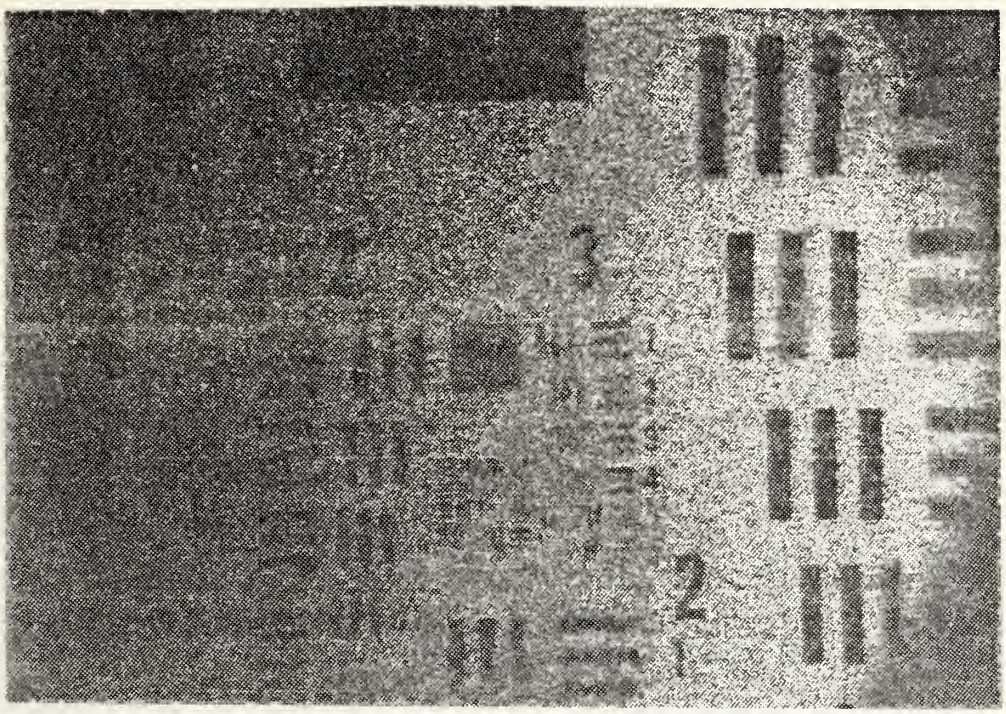

Figure 19. Kodak Panatomic X 1:1/5x of Hologram #74 w/Milar

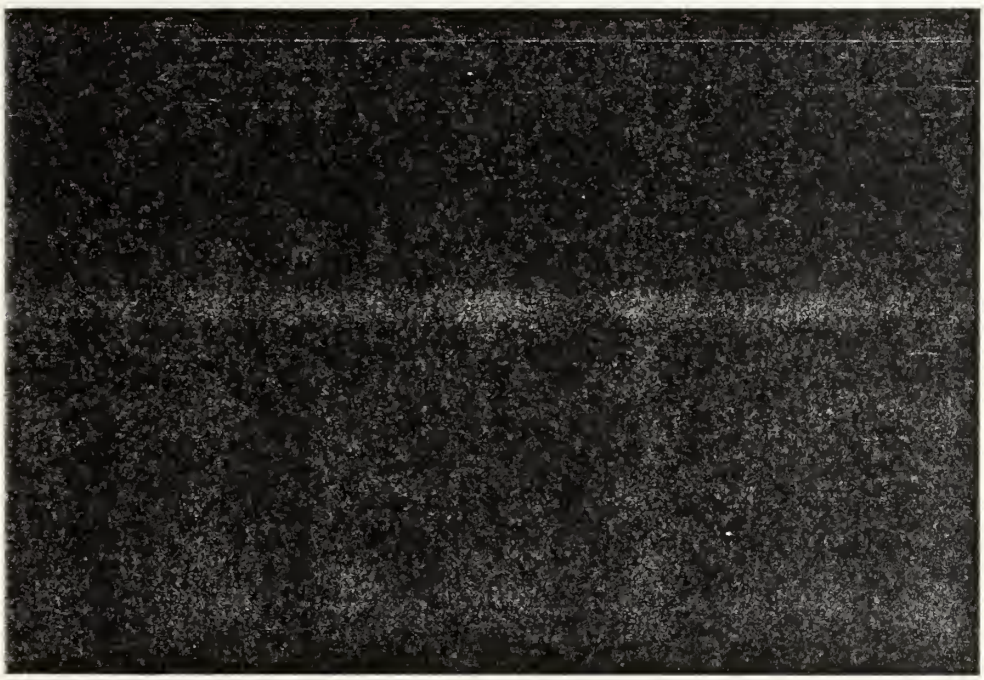

Figure 20. Kodak Kodachrome 25 1:1/20x of Hologram #74 w/Milar

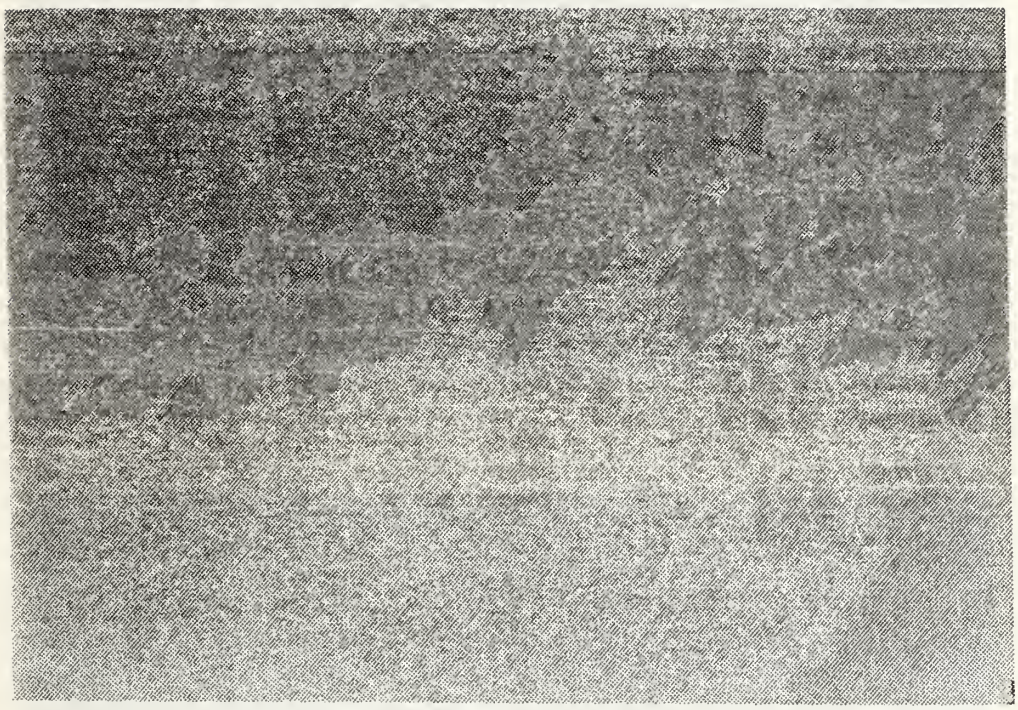

Figure 21. Kodak Panatomic X 1:1/20x of Hologram #100 w/Milar

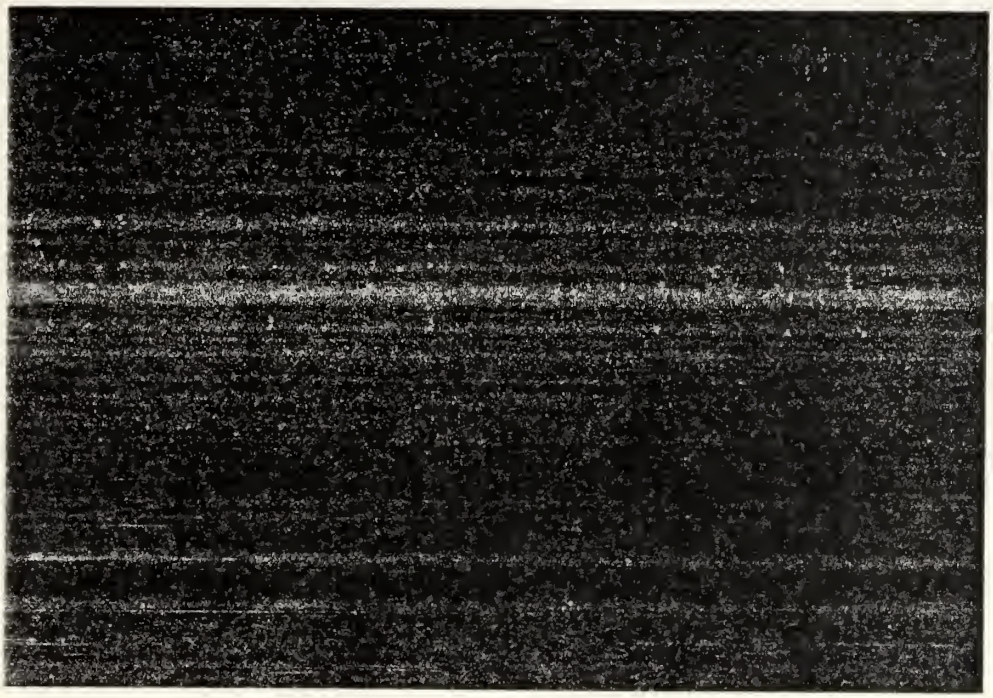

Figure 22. Kodak Ektachrome 400 1:1/20x of Hologram #46 w/Milar

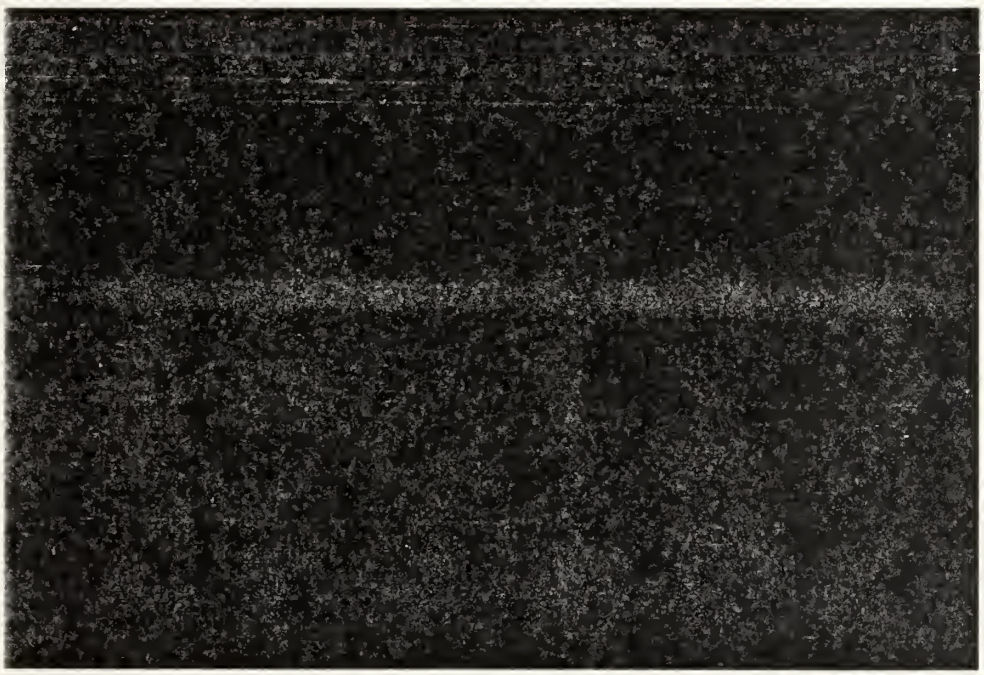

Figure 23. Kodak Kodachrome 25 1:1/20x of Hologram #46 w/Milar

enhanced the inherent speckle, reducing its overall resolution. No advantages were observed when the faster films were used.

The major problem that contributed to uncertainties throughout the experiment was the lack of proper focusing at higher magnifications. The extremely shallow depth of field coupled with the limited light available at the higher magnifications prohibited distinguishing between focusing errors and lack of the films resolution or speckle suppression method contribution. Exact focus could not be maintained spatially over the whole picture or from shot to shot. The difference between what was seen with the eye at the microscope and what was recorded on film was at times as much as 10μm.

Varying the lenses to produce magnification changes showed that ultimate resolution was not increased significantly (Figures 22, 24, and 25). Although some gains were possible in select pictures, the problem of obtaining proper focusing prevented any conclusive results from being made. Photographic enlargements of the pictures taken at the lower magnifications resulted in resolutions equal to those obtained when the microscope was used for magnification (Figure 26).

2. Milar Disk

The biggest gains in resolution were obtained using the milar disk (Figures 27 and 28, with milar rotating and not rotating, respectively). Differences exceeded 15μm in resolution capability.

3. Varying Aperture

The results of the attempt to change the speckle pattern by varying the objective aperture throughout an exposure proved inconclusive. The large magnification of the objective lens coupled with the

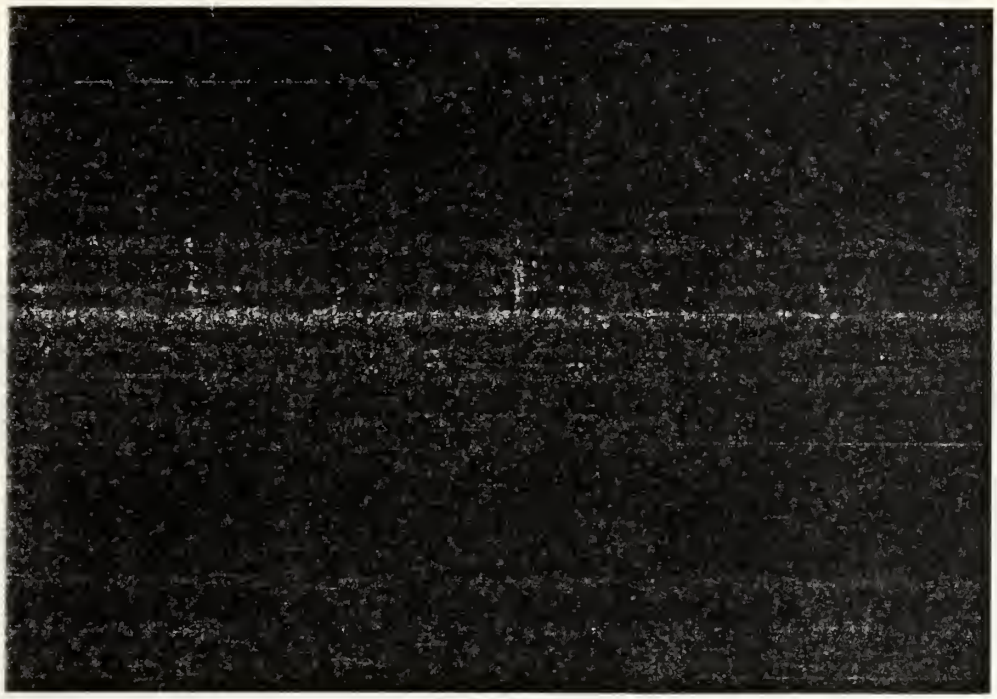

Figure 24. Kodak Ektachrome 400 1:1/5x of Hologram #46 w/Milar

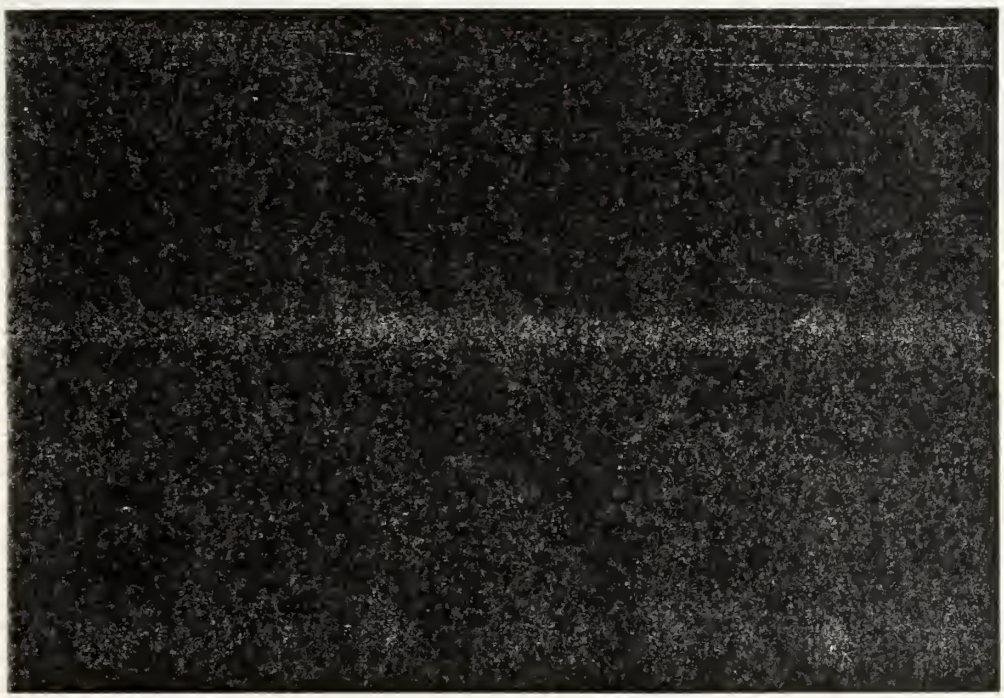

Figure 25. Kodak Ektachrome 400 1:1/10x of Hologram #46 w/Milar

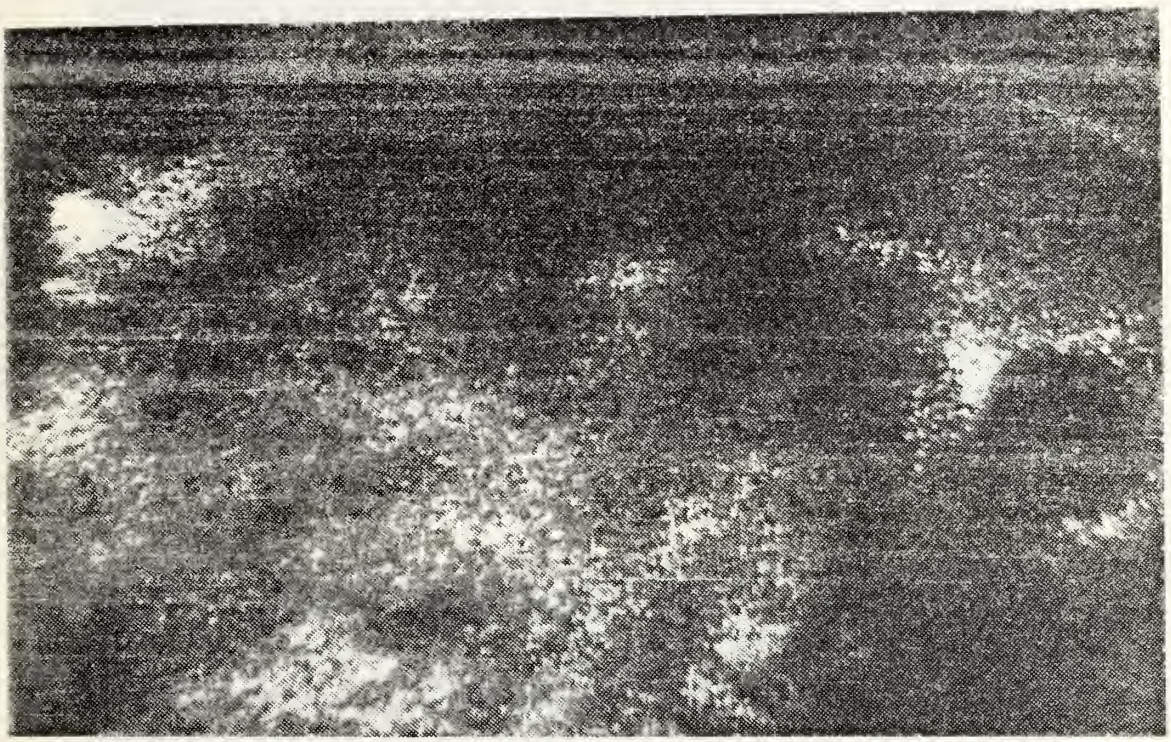

Figure 26. Kodak Panatomic X 1:1/5x of Hologram #74 w/Milar (2x Enlargement)

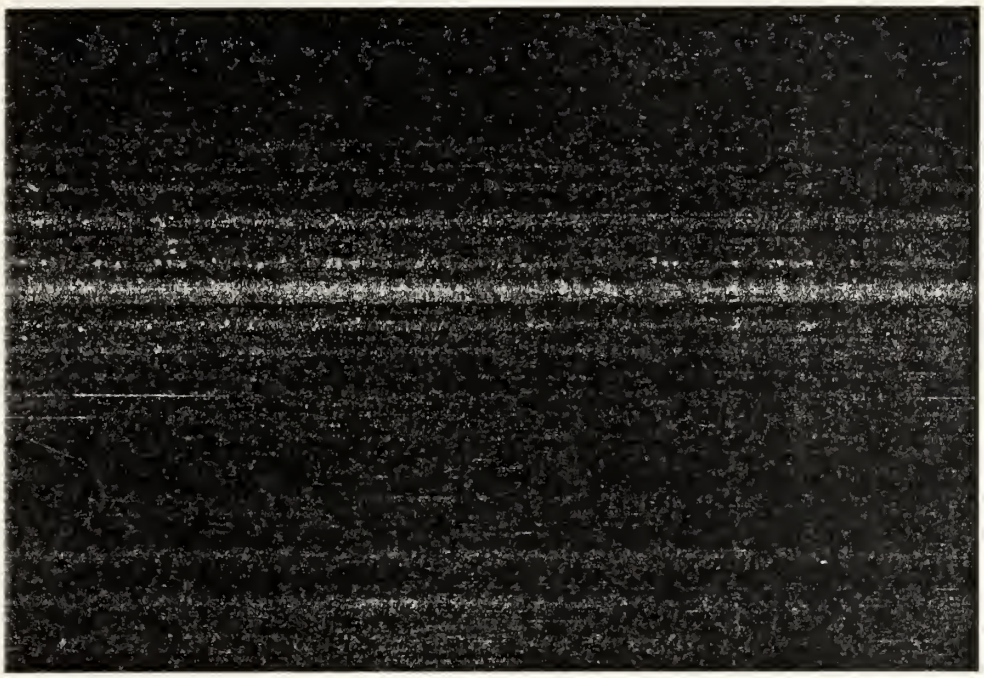

Figure 27. Kodak Kodachrome 25 1:1/5x of Hologram #74 w/Milar

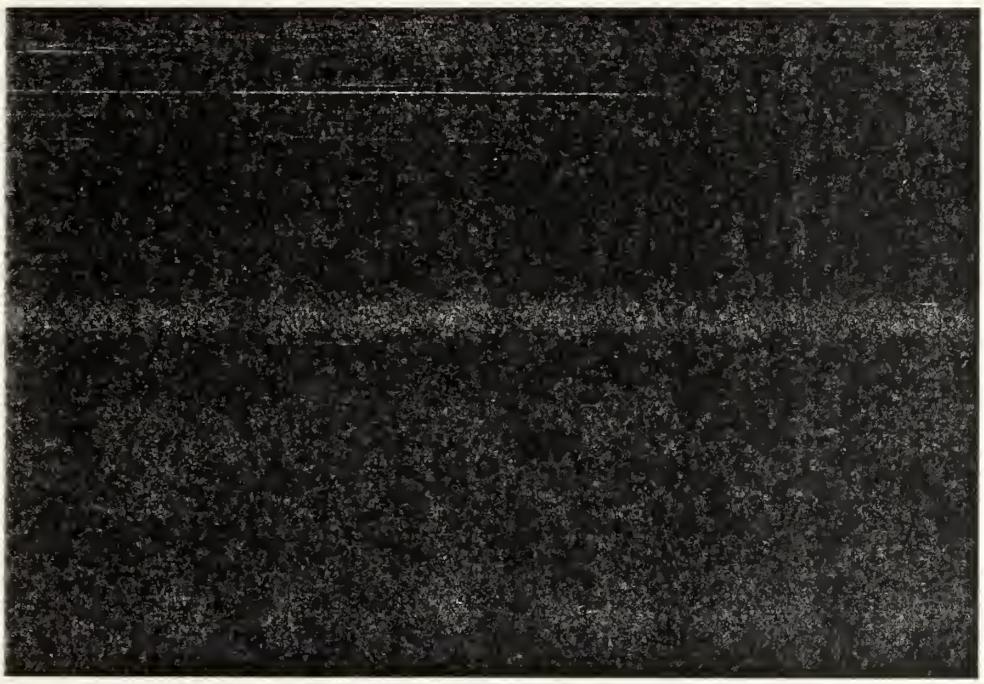

Figure 28. Kodak Kodachrome 25 1:1/5x of Hologram #74 w/o Milar

eyepiece lens (total of 50x) produced focusing problems that tended to cancel any gains derived from varing the speckle pattern.

4. Vibrating Diffuser

The vibrating diffuse plate did not contribute significantly to any increased resolution capability. Although some gain in resolution was realized with the vibrating ground glass plate it did not approach that obtained using the milar disk. The amplitude of the vibrations were considered inadequate to provide the necessary motion. When the opal glass was used in the vibrator it was too opaque to permit photographic recording. To boost the beam power at the opal plate the spatial filter and collimator were removed to take advantage of the reduced far field beam diameter, with negative results. Proper collimation still was necessary to avoid deterioration of the reconstructed image resolution.

5. Rotating Diffuser Plate (Illumination)

The rotating diffusing disk placed in the object beam did not produce the expected shift in speckle pattern. At 3000 rpm no noticeable difference in resolution was recorded. At 5520 rpm the speckle pattern remained appreciably the same with a deterioration in resolution of 10μm. Both runs were made using opal glass.

IV. RECOMMENDATIONS

To benefit from the use of higher magnification lenses in the microscope the focusing/depth of field problems needs to be addressed. By switching to a phase recording medium vice the absorption type presently used, higher diffraction efficiencies (30% greater) can be realized [Ref. 15]. This can be done by replacing the developed silver in the absorption hologram emulsion with transparent silver salts in a process referred to as bleaching, allowing an increase of light intensity in the real image, thus providing greater light levels at higher magnifications.

A finer adjustment on the microscope vernier is required at the depth of field present in the holograms produced from the holocamera system (described earlier). An alternative would be to reduce the aperture in the holocamera box by removing the assisting lens. A trade-off with increased speckle size will be necessary.

The aperture varing technique indicated some gain was possible, but at the lower magnifications. Isolating the aperture device from the objective lens may produce more satisfactory results.

A further technique is suggested by this investigation. The development of a holographic filter where the existing speckle pattern is recorded separately from the speckle and particles (or resolution target). This filter could then be used as a positive filter in reconstruction. Some gain may also be realized by using such a filter to produce a reference beam of the real speckle image. The projected real

image produced by retro-illuminating the speckle recording could in turn be used as a reference beam to retro-illuminate the hologram of the particles (or resolution target).

LIST OF REFERENCES

1. Hill, P. G., and Peterson, C. R., Mechanics and Thermodynamics of Propulsion, Addison Wesley Publishing Company, 1965.

2. Geisler, R. L., "Summary Report on 1977 JANNAF Aluminum Combustion Workshop", held at Hercules, Inc., 10-11 May 1977, Magna, UT.

3. Diloreto, V. D., "An Experimental Study of Solid Propellant Deflagration Using High Speed Motion Pictures and Postfire Residue Analysis", Engineer's Thesis, Naval Postgraduate School, June 1980.

4. Karagounis, S. G., "An Investigation of Particulate Behavior in Solid Propellant Rocket Motors", Engineer's Thesis, Naval Postgraduate School, June 1981.

5. Gillespie, T. R., "Holographic Investigation of Solid Propellant Particulates", Master's Thesis, Naval Postgraduate School, December 1981.

6. Thomson, B. J. et al, "Application of Hologram Techniques to Particle Size Analysis", Applied Optics, Vol 6, No. 3, March 1967.

7. Trolinger, J. D., and Field, D., "Particle Field Diagnostics by Holography", AAIA-80-0018, January 1980.

8. Wuerker, R. F., and Briones, R. A., "Operation Manual for the Lens-Assisted Multipulse Holocamera with Reflected Light-Option", AFRPL-TM-78-12, July 1978.

9. Unterseher, F., et al, Holography Handbook, P. 323, Ross Books, 1982.

10. Collier, R. J., et al, Optical Holography, Chapter 1.9, Academic Press, 1971.

11. IBID, Chapter 1.4.

12. Unterseher, F., op. cit., p. 329.

13. Smith, H. M., Principles of Holography, Second Edition, Chapter 2.3, John Wiley & Sons, 1975.

14. Unterseher, F., et al, op. cit.

15. Collier, R. J., op. cit.

16. IBID, Chapter 8.12 and p. 199-203.

17. IBID, Chapter 10.

18. IBID.

19. Smith, H. M., op. cit.

20. Wuerker, R. F., and Briones, R. A., op. cit.

21. Briones, R. A., and Wuerker, R. F., "Instruction Manual for the Improved Ruby Laser Holographic Illuminator", AFRPL-TM-78-11, July 1978.

22. Thomson, et al, op. cit., p. 1.

23. Briones, R. A., and Wuerker, R. F., "Application of Holography to the Combustion Characterization of Solid Rocket Propellants Final Report", p. 26, AFRPL-TR-77-90, 1978.

24. IBID.

25. Collier, R. J., op. cit., Chapter 10.1.1, p. 266.

26. IBID, Chapters 9 and 10.

27. Gillespie, T. R., op. cit., p. 26.

28. "Model 165 Ion Laser with Model 265 Power Supply, Instruction Manual", Spectra-Physics Pub.

29. "Model 332, 336, 338 Telescope and Spatial Filters, Instruction Manual", Spectra-Physics Pub.

30. Collier, R. J., op. cit., p. 197, Figure 8.14.

31. IBID, Chapter 10.8.1.

32. Cramer, R. G., "Particle Size Determination in Small Solid Propellant Rocket Motors Using the Diffractively Scattered Light Method", Aeronautical Engineer's Thesis, Naval Postgraduate School, October 1982.

33. Hansen, B. J., "Automatic Control and Data Acquisition System for Combustion Laboratory Applications", Aeronautical Engineer's Thesis, Naval Postgraduate School, October 1982.

INITIAL DISTRIBUTION LIST

		No. Copies
1.	Defense Technical Information Center Cameron Station Alexandria, Virginia 22314	2
2.	Library, Code 0142 Naval Postgraduate School Monterey, California 93940	2
3.	Department Chairman, Code 67 Department of Aeronautics Naval Postgraduate School Monterey, California 93940	1
4.	Professor D. W. Netzer, Code 67 Nt Department of Aeronautics Naval Postgraduate School Monterey, California 93940	2
5.	Lt. Marcus A. McInnis, USN 31 Allen Street Wilton, Maine 04294	2

200111

Thesis
M189465 McInnis
c.1 Optimization of a holographic reconstruction process for combustion phenomena.